

# RESULTS FROM MINIBOONE

BYRON P. ROE

For the MiniBooNE Collaboration

*Department of Physics, University of Michigan 450 Church Street  
Ann Arbor, MI 48109-1040, U.S.A.*

E-mail: byronroe@umich.edu

## ABSTRACT

Recent results from MiniBooNE are described. These include neutrino oscillation results, low energy anomaly, and neutrino/antineutrino cross sections.

### 1. The MiniBooNE Experiment

MiniBooNE was proposed in Summer 1997 to examine the result obtained in the LSND experiment. MiniBooNE has been running since 2002. The LSND experiment<sup>1)</sup> presented a  $3.8 \sigma$  signal for  $\bar{\nu}_\mu \rightarrow \bar{\nu}_e$  oscillations with  $\Delta m^2$  of the order of  $1 \text{ eV}^2$  and  $\sin^2 2\theta = 0.26 \pm 0.08$ . This result is incompatible with the results obtained for solar and atmospheric neutrinos in the framework of the three-neutrino standard model.

MiniBooNE makes neutrinos using the Fermilab Booster 8 GeV proton beam incident on a 71 cm long beryllium target inside of a toroidal focusing horn. Up to  $4 \times 10^{12}$  protons are contained within a  $\sim 1.6 \mu\text{s}$  beam spill at a rate of up to 4 Hz. Positively charged pions and kaons are focused into a 50 m long, 91 cm radius decay region. (See Figure 1.)  $L/E$  for MiniBooNE is quite similar to that for LSND, but the MiniBooNE mean neutrino beam energy of about 800 MeV is far greater than the LSND energy of about 50 MeV, resulting in very different systematics for the two experiments.

The first MiniBooNE oscillation result was based on an exposure of  $5.58 \times 10^{20}$  protons on target. Most of the neutrinos produced are  $\nu_\mu$ , but there is an intrinsic  $\nu_e$  fraction of about 0.5%, which comes from kaon and muon decay. About 39% of the neutrino interactions in the detector are charged-current quasi-elastic (CCQE) scattering, 16% are neutral-current (NC) elastic scattering, 29% are charged-current (CC) single pion production and 12% are NC single pion production.

The neutrino detector is located 541 m downstream of the beryllium target and is 1.9 m above the center of the beam line. The detector consists of a spherical tank with 610 cm inner radius containing 800 tons of pure mineral oil ( $\text{CH}_2$ ) of density  $0.86 \text{ g/cm}^3$  and index of refraction of 1.47. Fast charged particles produce both prompt, directional Cherenkov light and longer time constant scintillation light with a ratio of about 8:1. However, because of significant absorption and fluorescence, the ratio of prompt to delayed light at the detector photo-tubes is about 3:1. The detector consists of an inner spherical target region of radius 575 cm with 1280 equally-spaced inner-facing 8-inch photomultiplier tubes (PMT) providing 10% photocathode coverage.

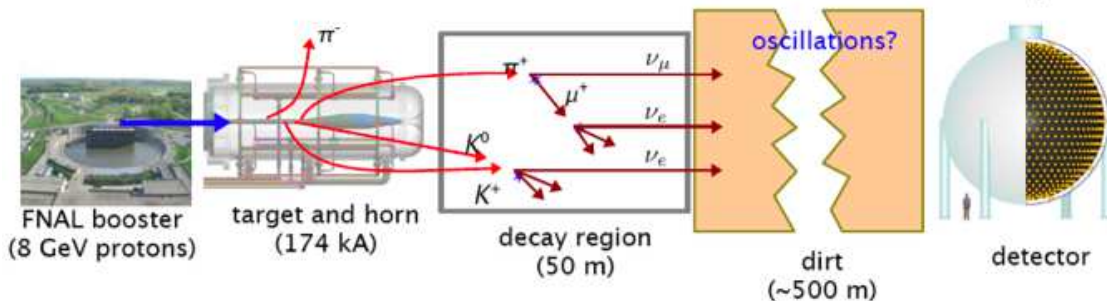


Figure 1: MiniBooNE beam

There is an optically isolated outer veto shield region 35 cm thick with 240 8-inch PMTs. The detector has been designed to detect and measure neutrino events in the energy range from 100 MeV to a few GeV. The event vertex, outgoing particle directions and visible energies are determined by event reconstruction, which also determines parameters allowing separation of  $\nu_e$  and  $\nu_\mu$  events.

## 2. Oscillation Analysis

In the initial MiniBooNE oscillation publication<sup>2)</sup>, two separate, but quite compatible, results coming from two different reconstruction-particle identification packages were presented. No LSND-like signal was seen. A first attempt to combine these two results to produce better limits has now been made and is shown in Figure 2. Below  $\Delta m^2$  of 1  $\text{eV}^2$ , the 90% CL limit is improved by 10-30%. This result used CCQE events above 475 MeV.

Global simultaneous fits to LSND, MiniBooNE, KARMEN2<sup>3)</sup> and Bugey<sup>4)</sup> have been performed<sup>5)</sup>. The results of each experiment were converted to a  $\chi^2$ . However, only  $\Delta\chi^2$  was available; the goodness of fit of individual experiments was not available for each case. Two-dimensional fits varying both oscillation parameters and one-dimensional fits, varying only  $\sin^2 2\theta$  were done. The fits were done using the prescription of Maltoni and Schwetz<sup>6)</sup>. For each  $\Delta m^2$ , the one-dimensional fit answers the question, “If this is the true  $\Delta m^2$ , what is the compatibility?” The two-dimensional fits are presented in Table 1. Using all four experiments, the maximum compatibility is 3.9%. If KARMEN2 is omitted, the maximum compatibility drops to 2.1%; the KARMEN2 experiment has the effect of diluting the results. If LSND is omitted, the maximum compatibility of the other three experiments is good, 25.4%. The limits of the Bugey experiment in the region below  $\Delta m^2 = 1 \text{ eV}^2$  are quite important for the global fit. The limits from the one-dimensional fits are quite comparable to those from the two-dimensional fits.

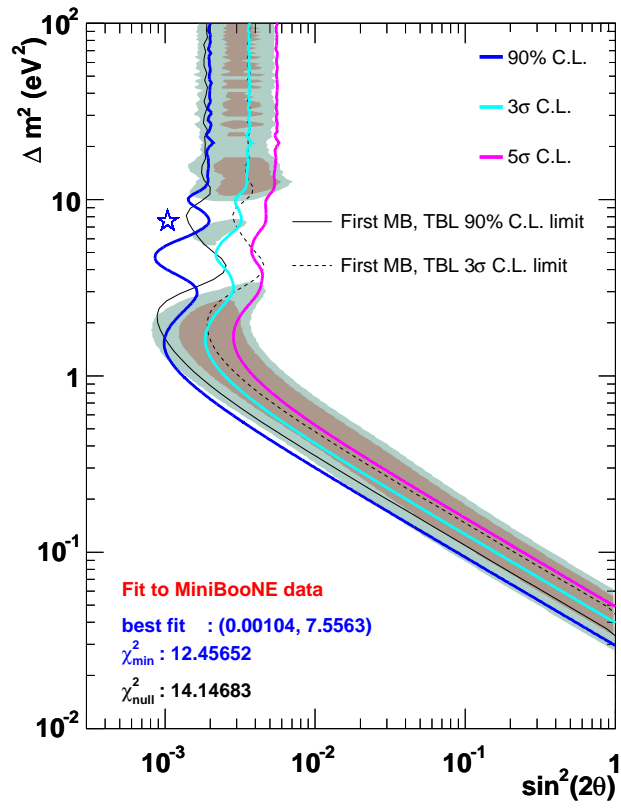


Figure 2: New MiniBooNE  $\nu_{\mu}-\nu_e$  oscillation limits combining the two independent reconstruction-particle identification methods.

Table 1: Maximum Compatibility for 2-D Global Fits to Experiments. The X indicates which experiments were included in the analysis.

LSND	KARMEN2	MB	Bugey	Max. Comp. (%)	$\Delta m^2$	$\sin^2 2\theta$
X	X	X		25.4	0.072	0.26
X	X	X	X	3.94	0.24	0.023
X		X		16.0	0.072	0.26
X		X	X	2.1	0.25	0.023
	X	X		73.4	0.052	0.15
	X	X	X	27.4	0.22	0.012

### 3. Low Energy Anomaly

In the MiniBooNE oscillation paper<sup>2)</sup>, the  $\nu_e$  CCQE energy spectrum from 300 to 475 MeV was found to have an excess of  $96 \pm 17 \pm 20$  events above that predicted from the null oscillation fit. No oscillation parameters fit the entire spectrum. Parameters which come close to fitting the low energy data predict too many high energy events. A number of studies of these low energy events are ongoing; it is hoped that a complete update will be available in Summer 2008. A status report on these studies is given below. None of the effects examined are expected to have any appreciable effect above 475 MeV.

The analysis has been extended down to the  $\nu_e$  CCQE energy region of 200-300 MeV, where an anomaly is also seen, similar in size to that in the 300-475 MeV region. Above 475 MeV there is essentially no excess,  $22 \pm 19 \pm 35$  events.

- No evidence of instrumental background has been found. Spatial and angular distributions of events within the detector are as expected as are event timings. Energy calibrations are done with data as described in the initial oscillation publication.
- The two reconstruction, particle identification packages give consistent analyses.
- Particle identification studies indicate that the excess is completely consistent with being electrons or gamma rays. (MiniBooNE cannot distinguish an electron track from the electron-positron pair resulting from gamma ray conversion.)
- NC events producing an excited nucleon  $\Delta$ , usually decay by  $\pi^0$ -nucleon, but occasionally by  $\gamma$ -nucleon, a  $\Delta$ -radiative decay. This latter decay emulates a  $\nu_e$

CCQE event. The  $\pi^0$ -nucleon events have been measured in the detector. This measurement calibrates the number of  $\Delta$ -radiative decays since the branching fraction for the mode is known and corrections for nuclear and threshold effects can be calculated.

- Neutrino events occurring in material outside the detector can produce  $\pi^0$ 's. If one of the decay gamma rays enters the detector it can simulate a  $\nu_e$  CCQE event. The gamma rays tend to be of low energy. Since the gamma conversion length is short, 70 cm, the extrapolated path length back to the detector wall tends to be short. By selecting events with short extrapolated length, these events can be enhanced and the size of the effect calibrated.
- An energy dependent cut on the backward extrapolated path length of the events is now being implemented. This has the effect of reducing the number of “dirt” events with only minor loss of signal.
- Various effects can cause events with an outgoing muon or pion to look like  $\nu_e$  CCQE events. For example, a preprint<sup>7)</sup> suggested that muon bremsstrahlung might be a cause of the anomaly. However, for 83% of the events with an outgoing muon, the muon decay is detected. These events appear as two sub-events with a time delay that of the muon decay time. By eliminating the muon decay sub-event, a sample of guaranteed muons or pions is obtained. These events are then reprocessed through the reconstruction and particle identification steps to see whether any pass the  $\nu_e$  CCQE criteria. The fraction of the anomaly due to these events is about 2%<sup>8)</sup>.
- If one of the gamma rays from  $\pi^0$  decay is absorbed by means of a photo-nuclear process, the remaining gamma ray may appear to be a  $\nu_e$  CCQE event. Photo-nuclear processes were not included in the version of GEANT originally used. Using data from other experiments, the cross section for this process as a function of energy was estimated as was the effect of extra final state particles. This process reduces the anomaly. The size of the reduction and the systematic errors on it are still being calculated.
- A more comprehensive study of hadronic errors and a better handling of  $\pi^\pm$  interactions is ongoing. It is expected that this will result in a reduction of the anomaly.
- A better handling of the  $\pi^0$  background calculation is underway. This will reduce the anomaly.
- Improved measurements of neutrino induced  $\pi^0$ 's is expected to increase the anomaly.

- An improvement in the handling of beam  $\pi^+$  production uncertainties is in the process of being implemented. The effect on the anomaly is uncertain.
- Examination of the anomaly in  $\bar{\nu}$  events will be done shortly. The fractions of various kinds of background in both samples is similar, except that the  $\bar{\nu}$  beam events have a larger fraction of intrinsic  $\nu_e$  events (2.45% vs 0.5% for events in the  $\nu$  beam). Different hypotheses for the excess, however, can have measurably different effects in the two samples.

### 3.1. Some Theoretical Suggestions for Causes of the Anomaly

One suggestion is a new process within the standard model, an axial anomaly<sup>9)</sup>. This suggestion involves a triangle diagram. A nucleon emits an  $\omega$  which goes to one vertex of the triangle. The neutrino emits a  $Z$  which goes to the second vertex of the triangle, and a gamma ray is emitted from the third vertex. The low energy limit cross section with no nucleon recoil is

$$\sigma = \frac{\alpha g_\omega^4 G_F^2}{480\pi^6 m_\omega^4} E_\nu^6 = 2.2 \times 10^{-41} \left( \frac{E_\nu}{\text{GeV}} \right)^6 \left( \frac{g_\omega}{10} \right)^4. \quad 1$$

The cross section is expected to saturate at higher energies. A more detailed calculation of the expected gamma ray energy and angular distribution using a Monte Carlo calculation from the complete amplitude is now underway. Normalization is a problem since  $g_\omega$  can vary by a factor of about three, from 10 to 30, and it appears in the cross section to the fourth power.

Another suggestion<sup>10)</sup> involves a new light gauge boson called a paraphoton. There is an MSW-like potential in matter which affects low energy neutrino oscillations. It makes LSND and MiniBooNE results compatible and obtains a low energy anomaly about 40% of that seen in MiniBooNE. The paraphoton has a mass of  $\sim 10$  KeV. (It needs to be short range to avoid fifth force measurements). It has a very low coupling strength to B-L with  $g^2/e^2 \sim 10^{-9}$ , which was thought to make it undetectable. However, MiniBooNE has about  $6 \times 10^{20}$  protons on target. Two back-of-the-envelope calculations indicate that there might be 10-20 events in the very forward direction, looking like an anomalous  $\nu_e$ - $e$  scattering cross section. A paraphoton would be produced by hadronic bremsstrahlung of the incident proton beam and seen in the detector by producing an electron-positron pair. Examination of our present data is underway. More events will be needed for a definitive answer, but for this process, the  $\bar{\nu}$  beam is as good as the  $\nu$  beam. This calculation indicates that

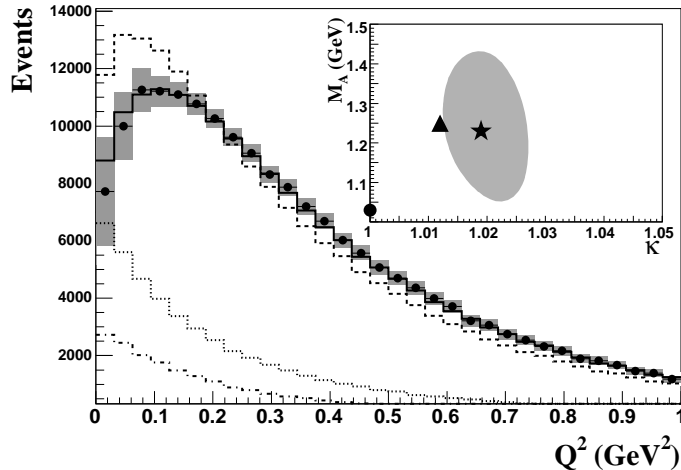


Figure 3: Reconstructed  $Q^2$  for  $\nu_\mu$  CCQE events including systematic errors. The simulation before (dashed) and after (solid) fitting, is normalized to the data. The dotted (dot-dash) curve shows backgrounds that are not CCQE (“CCQE-like”). The inset shows the  $1\sigma$  contour for the best-fit parameters (star), along with the starting values (circle), and the fit results after varying the background (triangle).

MiniBooNE is capable of doing very sensitive searches for a variety of rare processes.

## 4. Neutrino and Anti-Neutrino Cross Sections

### 4.1. $\nu_\mu$ CCQE Cross Section

The  $Q^2$  dependence of the  $\nu_\mu$  CCQE events has been fit<sup>11)</sup> using a relativistic Fermi gas model. 193,709 events pass the MiniBooNE  $\nu_\mu$  CCQE criteria. The binding energy and the Fermi momentum were taken from electron scattering data and the effective axial mass  $M_A^{\text{eff}}$  and Pauli blocking parameter  $\kappa$  were fitted.  $M_A^{\text{eff}} = 1.23 \pm 0.20$  GeV and  $\kappa = 1.019 \pm 0.011$ .  $M_A^{\text{eff}}$  is larger than the values found in previous, lower statistics, experiments, but is in agreement with the K2K result<sup>12)</sup>. These are all effective values since the Fermi gas model is a poor approximation; a better calculation is needed. The  $Q^2$  distribution is shown in Figure 3.

### 4.2. $\nu_\mu$ NC Elastic Cross Section

The present results are from a 10% sample of our data. The flux integrated cross section is  $8.8 \pm 0.6(\text{stat}) \pm 2.0(\text{syst}) \times 10^{-40}$  cm<sup>2</sup>, and the measured axial mass is

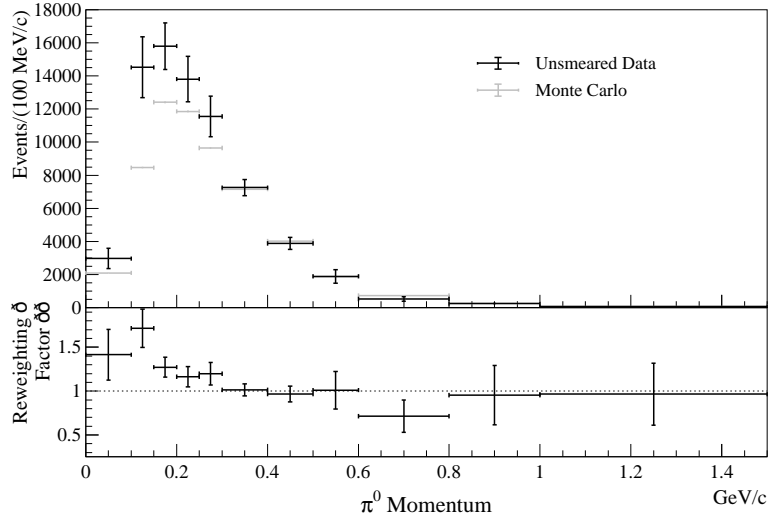


Figure 4: NC  $\pi^0$  Reconstruction Unsmearing. Top: Results of the  $\pi^0$  unsmearing in bins of momentum. Dark points are unsmearred data, light points are uncorrected Monte Carlo. Bottom: Re-weighting function.

$1.34^{+0.38}_{-0.25}$  GeV. The full data set is now under analysis.

#### 4.3. NC and CC $\pi^0$ Events

It is important to calibrate the NC  $\pi^0$  event sample. If one  $\pi^0$  decay gamma rays is lost, the remaining gamma ray is a background for our oscillation analysis. Radiative nucleon resonance decays form another background to  $\nu_e$  events. The NC  $\pi^0$  data events were compared with Monte Carlo predictions. The Monte Carlo cross sections were corrected by re-weighting Monte Carlo events to match the data. This was important both for the MiniBooNE oscillation analysis and for understanding the low energy anomaly. Figure 4 shows a comparison of unsmearred data events and the unmodified Monte Carlo events as a function of  $\pi^0$  momentum as well as the needed re-weighting factor.

This NC event sample can also be examined to find the fraction of events not going through a nucleon resonance, but going coherently. This fraction was measured to be  $19.5 \pm 1.1(\text{stat.}) \pm 2.5(\text{syst.})\%$ , which is considerably below the 30% prediction of Rein and Sehgal<sup>13)</sup> as implemented in the NUANCE Monte Carlo<sup>14)</sup>.

The CC event sample has a gamma-gamma effective mass distribution in good agreement with Monte Carlo expectations. This sample of events has no coherent



contribution.

#### 4.4. $\bar{\nu}$ NC $\pi^0$ Cross Section

The data and Monte Carlo agree very well in the shape of the gamma-gamma effective mass. When a fit is made for resonant, coherent, and background fractions, the coherent fraction is again considerably less than predicted by Rein and Sehgal.

#### 4.5. $\nu_\mu$ CC $\pi^+$ Events from the $\bar{\nu}$ Beam

This cross section provides a direct measurement of the rate and energy dependence of  $\nu$  backgrounds in the  $\bar{\nu}$  beam. In addition, most of the  $\nu$  production comes from decays of very forward  $\pi^+$ , since, if they enter the focusing horn, they are bent away from the detector. This allows a check of the  $\pi^+$  production at angles below that at which data exists. Results are shown in Figure 5.

## 5. References

- 1) C. Athanassopoulos *et al.*, *Phys. Rev. Lett.* **75** (1995) 2650; 77, (1996) 3082; 81, (1998) 1774; A. Aguilar *et al.*,
- 2) A. A. Aguilar-Arevalo *et al.*, *Phys. Rev. Lett.* **98** (2007) 231801. *Phys. Rev. D* **64** (2001) 112007.
- 3) B. Armbruster *et al.*, *Phys. Rev. D* **65** (2002) 112001.
- 4) B. Achkar *et al.*, *Nucl. Phys.* **B434** (1995) 503.
- 5) A. A. Aguilar-Arevalo *et al.*, arXiv:0805.1764 (2008).
- 6) M. Maltoni and T. Schwetz, *Phys. Rev. D* **68** (2003) 033020.
- 7) A. Bodek, arXiv:0709.4004 (2007).
- 8) MiniBooNE Collaboration, arXiv:0710.3897 (2007).
- 9) J. A. Harvey, C. T. Hill, and R. J. Hill, arXiv:0708.1281 (2007), 0712.1230 (2007).
- 10) A. Nelson and J. Walsh, arXiv:0711.1363 (2007).
- 11) A. A. Aguilar-Arevalo *et al.*, *Phys. Rev. Lett.* **100** (2008) 032301.
- 12) R. Gran *et al.*, *Phys. Rev. D* **74** (2006) 052002.
- 13) D. Rein and L. M. Sehgal, *Nucl. Phys.* **B223** (1983) 29.
- 14) D. Casper, *Nucl. Phys. Proc. Suppl.* **112** (2002) 161.

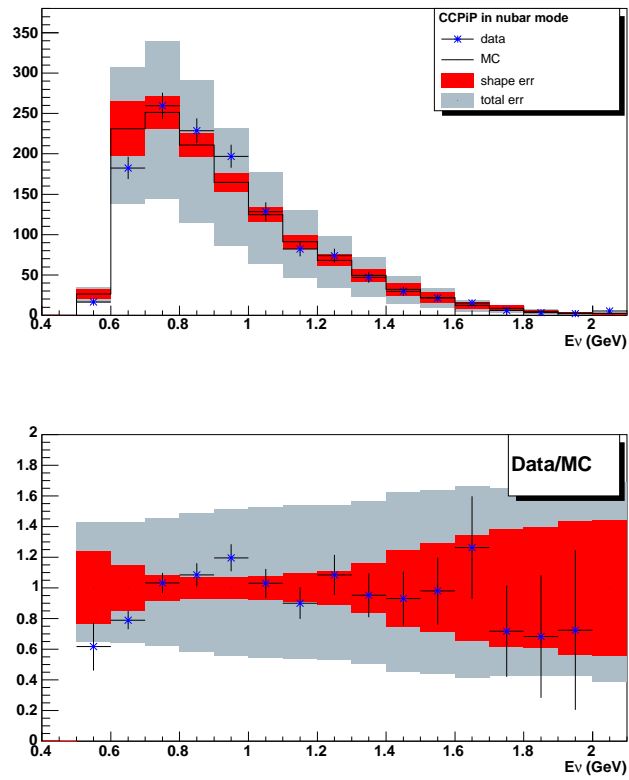


Figure 5: Top: Data (dots) and Monte Carlo (solid line) for  $\nu_\mu$  events giving a  $\pi^+$  seen in the  $\bar{\nu}$  beam. The bars indicate shape and total errors. Bottom: Ratio of data to Monte Carlo.